Studia Geotechnica et Mechanica, Vol. XXX, No. 1–2, 2008

A MODEL FOR THE FORECASTING OF THE PROPAGATION OF TECHNOLOGICAL IMPACTS

MACIEJ GRYCZMAŃSKI, MAŁGORZATA JASTRZĘBSKA, MARIAN ŁUPIEŻOWIEC

Department of Geotechnics, Silesian University of Technology,
ul. Akademicka 5/214, 44-100 Gliwice, Poland. E-mail: marian.lupiezowiec@polsl.pl

Abstract: This paper deals with the application of an elasto-viscoplastic version of the NAHOS model built in the Department of Geotechnics, Silesian University of Technology. The model has been developed since 1997. It is able to realistically describe the material response to complex load paths. It can also describe non-linear characteristics within the small strain range and the effect of the rate on the process. The elastoplastic NAHOS model was presented in detail at the Polish–French colloquium in Wrocław, Poland, in 2003. The model is based on the results of cyclic triaxial tests, for the purposes of this article performed on kaolin samples without drainage, following back pressure saturation and then isotropic consolidation. The paper quotes these results and briefly presents model equations and the procedure of model's implementation for the title problem.

1. INTRODUCTION

Technological impacts discussed in the paper are powerful vertical impulses transferred to the ground surfaces during the processes of driving piles and steel sheet piles, forming stone columns by the dynamic replacement or Franki's methods, compacting soils by heavy tamping, etc. There are certain properties which can be identified for the above mentioned methods. They have short-time effect, namely, they are limited to a small number of cycles. The vibrations which are propagated into the surrounding soil in the form of mechanical waves are subject to strong viscoplastic dumping. As a result of dumping, not only is the effect limited to a small number of cycles, but the vibration amplitude in the successive cycles is considerably reduced.

This unsteady process can be realistically described in terms of mathematics by means of the initial-boundary value problem of dynamics. For this to be achieved an advanced kinematic hardening elasto-viscoplastic model for soil needs to be applied. It is the authors' belief that the NAHOS model meets the requirements. Naturally, as the process is reduced to a small number of cycles, the incremental FEM analysis of the problem becomes quite feasible.

It seems that a reasonable calibration (parametric identification) of the model may prove the most difficult task. An adequate starting point may be required if the optimal evaluation of the dynamic effect of engineering works on the structures of neighbouring buildings or other engineering objects as well as on people remaining in close vicinity is to be achieved.

2. MODEL DESCRIPTION

The model has been created based on the assumption that the total strain ε decomposes into elastic part ε^e and inelastic part ε^{vp}. The elasticity law is identical to that in the elastoplastic version of the model. The bounding surface, which separates normal consolidation (points on the surface) from preconsolidation (points inside the surface), is defined as follows:

$$F(\sigma', p_c, \dot{p}_c) = q'^2 + M^2 p'(p' - (p_c + A\dot{p}_c)) = 0 \,. \tag{1}$$

Equation (1) depends on the hardening parameter (preconsolidation pressure) p_c and the rate at which it changes. It is a generalised form of the yield condition for the modified clay model. Such form of the equation enables modelling of the influence of the process rate (HEERES and de BORST [4]). The inelastic strain rate is determined by the plastic flow rule which assumes the direction of the strains as normal to the bounding surface (the associated flow rule). Evolutions of the bounding surface (extending or contracting) are governed by the viscoplastic isotropic hardening rule:

$$\dot{p}_c = \frac{1+e}{\lambda - \kappa} p_c (\dot{\varepsilon}_v^{vp} + \xi \exp(-\xi_1 \varepsilon_s^{vp}) \dot{\varepsilon}_s^{vp}) - B \exp\left(\frac{q}{q_0}\right) p_c \,. \tag{2}$$

Equation (2) expresses the preconsolidation pressure rate p_c as being dependent on volumetric and shear strains (WILDE [10]) and also on the current state of preconsolidation pressure. Such a form of equation (2), proposed by DRAGON and MRÓZ [3], enables the description of the relaxation phenomenon. The values A and B in equations (1) and (3) are model parameters introduced by the author (comp. ŁUPIEŻOWIEC [9]).

The complexity of the system of differential equations (1) and (2) makes obtaining the closed form of the final incremental σ–ε relationship unfeasible.

It has been assumed that the yield surface inside the bounding surface is reduced to a single point, called the elastic centre S. Soil response to any loading path inside the bounding surface is described by the radial mapping rule (figure 1).

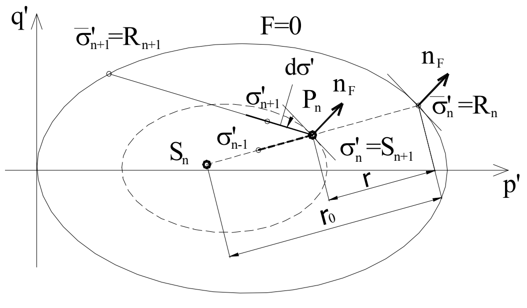

Fig. 1. The radial mapping rule

The hardening modulus at the point *P* is defined as follows:

$$K_P = K_R + H(\sigma', \varepsilon_v^{vp}, \varepsilon_s^{vp}) \cdot \frac{r}{r_0 - r}, \tag{3}$$

where:

$$K_R = \frac{\partial F}{\partial p_c} \left(\frac{\partial p_c}{\partial \boldsymbol{\varepsilon}^{vp}} \right)^T \left(\frac{\partial F}{\partial \sigma'} \right)$$

is the value of the hardening modulus in the reflecting point *R*, and

$$H = C \left(\frac{r}{r_0 - r} \right)^{\mu - 1}$$

is the hardening function. The proposed function *H* enables simulation of strong non-linearity within the small strain range.

The consistency condition that accounts for the above set of equations and

$$\left(\frac{\partial F}{\partial \sigma'} \right)^T \dot{\sigma}' + \frac{\partial F}{\partial p_c} \dot{p}_c + \frac{\partial F}{\partial \dot{p}_c} \ddot{p}_c = 0 \tag{4}$$

leads to constitutive equations:

$$\dot{\sigma}' = D \left(\dot{\varepsilon} - \dot{\Lambda} \frac{\partial F}{\partial \sigma'} \right), \tag{5a}$$

$$s\ddot{\Lambda} + h\dot{\Lambda} + c = 0, \tag{5b}$$

whose coefficients are defined as follows:

$$s = -M^4 p' A p_c \frac{1+e}{\lambda - \kappa} [2p' - (p_c + A\dot{p}_c)] - M^2 \frac{1+e}{\lambda - \kappa} p' A p_c \cdot 2q' \xi \exp(-\xi_1 \dot{\varepsilon}_s^{vp}),$$

$$h = -M^4 [2p - (p_c + A\dot{p}_c)]^2 K - 12Gq^2 - M^4 \frac{1+e}{\lambda - \kappa} [2p - (p_c + A\dot{p}_c)] p (p_c + A\dot{p}_c)$$

$$- M^2 \frac{1+e}{\lambda - \kappa} p \cdot 2q\xi \exp(-\xi_1 \varepsilon_s^{vp}) (p_c + A\dot{p}_c + Ap_c \dot{\varepsilon}_s^{vp})$$

$$- M^4 \frac{1+e}{\lambda - \kappa} p A p_c (2\dot{p} - \dot{p}_c - A\ddot{p}_c) - M^2 \frac{1+e}{\lambda - \kappa} A \cdot 2q p_c \xi \exp(-\xi_1 \varepsilon_s^{vp}) + C \left(\frac{r}{r_0 - r} \right)^{\mu},$$

$$c = KM^2 [2p' - (p_c + A\dot{p}_c)] \dot{\varepsilon}_V + 6q' G \dot{\varepsilon}_s - M^2 p' B (p_c + A\dot{p}_c).$$

Unlike in the DAFALIAS' and HERRMANN's proposal [2], the elastic centre S is not constant, but changes its location after each sharp bend of a stress path (figure 1). This can be described by the condition: $\mathbf{n}^T \cdot d\sigma' < 0$, where $\mathbf{n}$ is the unit vector normal to the bounding surface, and $d\sigma'$ is the stress increment. When the current point reaches the bounding surface, the further behaviour of the material is governed by formulas derived for normal consolidation.

3. LABORATORY TESTING OF SOILS

3.1. EQUIPMENT DESCRIPTION

To perform tests on kaolin samples a conventional triaxial apparatus was used. A triaxial cell contains internal tie bars and a rigid connection between the top cap and the loading piston. The diameters of top cap and pedestal are equal to that of the specimen. Strips of filter paper along specimen and porous stones, screwed onto the top cap and the bottom base, were used for drainage. The pressure chamber was filled with deaerated water.

Two different measurements of the axial deformation ε_1 were carried out:

• The internal axial deformation ε_1 on the lateral surface of the specimen, using two pairs of high-resolution submergible proximity transducers. The transducers were mounted at two positions, opposite to each other, around the specimen's diameter (figure 2). The range and the resolution of these transducers were 2.0 mm and 0.01%, respectively.

• The external axial deformation ε_1, using the external displacement gauge fixed on the loading piston.

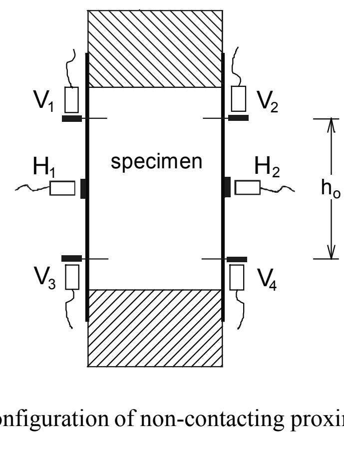

Fig. 2. Basic configuration of non-contacting proximity transducers

The lateral deformation ε_s was measured directly and locally, using a couple of proximity transducers placed in the central part of the specimen. The data reading took place at chosen time intervals.

3.2. TESTING PROCEDURE

The material used in this study came from the Porcelain Factory in Tulowice. Its basic properties are given in table 1. The soil tested exhibited great homogeneity of structure.

The triaxial tests were carried out on 50 mm diameter and 100 mm high specimens. Each specimen was fully saturated. At first, they were flushed with deaerated water. Next, a high back pressure was applied. The Bishop's *B*-values obtained equalled 0.98.

Table 1

Values of some physical properties and classification characteristics of Tulowice kaolin (JASTRZĘBSKA [6])

Specific gravity	G_S	g/cm^3	2.637	Skempton coefficient	A	–	0.52–0.60
Natural water content	w_n	%	33.4–37.7	Void ratio	e	–	0.956–1.098
Liquid limit	w_L	%	42.2	Clay fraction	CF	%	37.0–37.9
Plastic limit	w_p	%	20.0	Silt-size fraction	SF	%	53.7–56.3
Plasticity index	I_p	%	22.2	Effective angle of internal friction	ϕ'	°	25.0
Liquidity index	I_L	–	0.30–0.35	Poisson's ratio	ν	–	0.085

Following isotropic consolidation, undrained tests were carried out up to 15% of axial strain. The tests' conditions are specified in detail in table 2. For the purpose of model verification several series of tests have been performed. This is presented in detail in literature (JASTRZĘBSKA and STERNIK [8], JASTRZĘBSKA and ŁUPIEŻOWIEC [7]). Basic parameters of the laboratory research are given in table 2. For two selected tests (12–8 and 13–4c) the numerical simulation will be presented (figures 3 and 4).

Table 2

Test conditions of undrained cyclic triaxial compression test on Tulowice kaolin

Test No.	Type of test	OCR	Rate of ε_1 (mm/h)	u_b [kPa]	σ'_c [kPa]	B	e_0	$\varepsilon_{\text{unload'1}}$
12–2	CIU (10 cycles)	1.0	0.22	442	308	0.98	1.098	1.58
13–3			0.05	443	307	0.98	0.986	1.50
12–3	CIU (10 cycles)	2.8	0.22	441	309	0.98	1.041	1.62
13–4			0.05	441	309	0.98	0.956	1.38
12–8	CIU (monotonic)	14.5	0.22	342	408	0.99	0.955	–
13–4c			0.05	342	408	0.98	0.955	–

4. NUMERICAL SIMULATIONS

The numerical simulations of cyclic compression in a triaxial apparatus were performed using the Matlab program, which enabled the calculation of complex formulas and presentation of the results obtained in a simple way. In computation, the implicit predictor–corrector algorithm (HEERES and de BORST [4], ŁUPIEŻOWIEC [9]) was used to solve the constitutive relations (5).

The problem of the behaviour of isotropically consolidated samples was considered. The samples in question (and those uncompressed/additionally uncompressed into preconsolidation for the purpose of the analysis) were subsequently triaxially undrained loaded to reach $\varepsilon \approx 1.5\%$, exposed 10 times to unloading/loading process and finally undrained loaded to 15%. Because of isotropic stress and strain state, which occurs in a sample, the numerical analysis concerns only one isolated point. This assumption simplifies the analysis and it is no longer necessary to solve the whole bounding problem. The initial problem fulfils the laboratory tests' conditions described in the previous paragraph.

Numerical simulations were performed with the following values of the model parameters:

$$G = 40.0 \text{ MPa}, \quad M = 0.95, \quad \lambda = 0.30, \quad \kappa = 0.02, \quad e_0 = 0.75, \quad \xi = 2.0,$$

$$\xi_1 = 1.0, \quad A = 0.0005 \text{ h}, \quad B = 1 \cdot 10^{-7} \text{ 1/h}, \quad q_0 = 1.0 \text{ kPa}, \quad C = 5 \text{ MPa}, \quad \mu = 1.0.$$

The results of the numerical simulation are presented in figures 3 and 4, where the q–ε_s characteristics at different velocity of loading process are compared. Numerical results are compared with laboratory tests which were used for calibration and verification of the constitutive model.

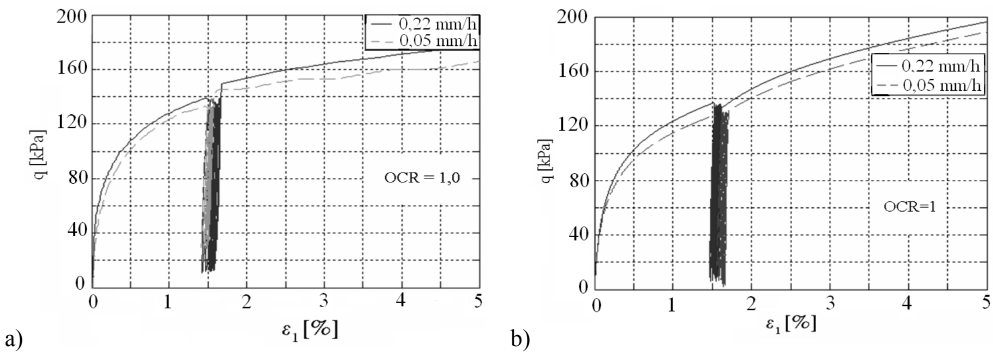

Fig. 3. Results of laboratory tests (a) and numerical simulations (b) ran on normally consolidated samples

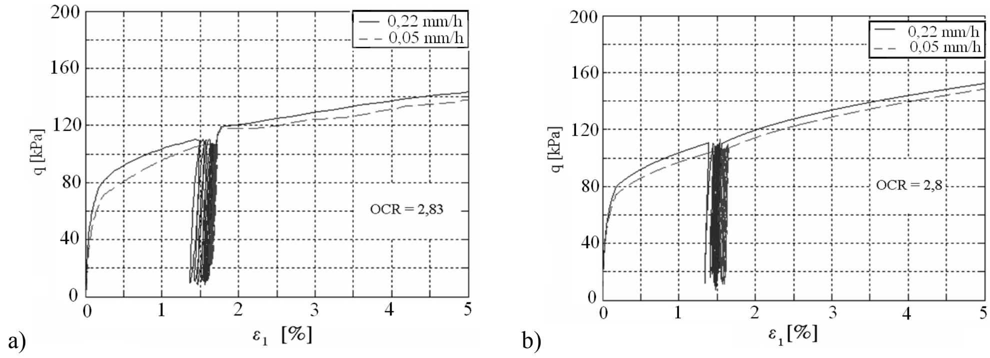

Fig. 4. Results of laboratory tests (a) and numerical simulations (b) ran on overconsolidated samples

5. COMMENTS ON THE APPLICATION OF THE MODEL IN THE ANALYSES OF THE PROPAGATION OF TECHNOLOGICAL IMPACTS

The results of the analysis of the elasto-viscoplastic model NAHOS show that the model responds adequately to cyclic loading paths and to the rate at which they change. It is therefore perfectly suitable for the analysis of the propagation of vibrations which are unsteady and subject to strong dumping, e.g., the technological impacts mentioned in the introduction.

The problem boils down to solving the nonlinear matrix equation of motion:

$$\mathrm{M}\cdot\ddot{\mathbf{u}}+\mathbf{K}(\boldsymbol{\sigma},\kappa,\dot{\kappa})\cdot\mathbf{u}=\mathbf{P}(t)\,, \tag{6}$$

where **M** is a mass matrix, **K** – a stiffness matrix, which is a function of the hardening parameter κ and its rate $\dot{\kappa}$, **P** – the input function, **u** – the displacement of the analysed structure.

To obtain the full specification and parametric identification of the model the adequacy of material functions dependent on the rate of strain within the high frequencies' range needs to be confirmed. This will be carried out during the next stage of the model implementation, within the framework of a project financed by the Polish Ministry of Science and Higher Education.

ACKNOWLEDGEMENT

This research was performed within the framework of the project No. 4 T07E 019 30 entitled "The modelling of the influence of technological impacts on neighbourhood", financed by the State Committee for Scientific Research.

REFERENCES

[1] ATKINSON J.H., BRANSBY P.L., *The mechanics of soils. An introduction to critical state soil mechanics*, McGraw-Hill, 1978.

[2] DAFALIAS Y.F., HERRMANN L.R., *A bounding surface soil plasticity model*, [in:] G.N. Pande and O.C. Zienkiewicz (eds.), *Soils under Cyclic and Transient Loading*, Proc. Int. Symp., Swansea, Balkema, Rotterdam, 1980, 335–345.

[3] DRAGON A., MRÓZ Z., *A model for plastic creep of rock-like materials accounting for the kinetics of fracture*, Int. J. Rock Mech. Sci. and Geomech., 1979, 16, 253–259.

[4] HEERES O., de BORST R., *A novel rate-dependent subloading model and its implicit integration*, European Conference on Computational Mechanics, Cracow, 2001.

[5] JASTRZĘBSKA M., *Calibrage d'un modèle d'argile à une surface au renforcement anisotrope non lineaire*, XII Colloque Franco-Polonais de Méc. de Sols et des Roches Appliq., Paris, 2000, 1.

[6] JASTRZĘBSKA M., *Identification parametrique et validation d'un modele d'argile preconsolidee elasto-plastique anisotrope non lineaire*, XII Colloque Franco-Polonais de Mécanique de Sols et des Roches Appliquée, Wrocław, 2004, 27, No. 1–2, 79–90.

[7] JASTRZĘBSKA M., ŁUPIEŻOWIEC M., *The effect of the rate on the cyclic strains in the cohesive soils in the light of theoretical and laboratory tests*, 16th International Conference on Soil Mechanics and Geotechnical Engineering, Osaka, 2005, 807–810.

[8] JASTRZĘBSKA M., STERNIK K., *Application of elasto-plastic model with anisotropic hardening to analysis of cyclic loading of cohesive soil*, International Conference on Cyclic Behaviour of Soils and Liquefaction Phenomena, Bochum, Germany, 2004.

[9] ŁUPIEŻOWIEC M., *Consistent viscoplastic model – conception and experimental verification*, II YGEC, Mamaia–Constanza, 2003, 13–14.

[10] WILDE P., *Two invariants dependent model of granular media*, Arch. of Mechanics, 1977, 29, 799–809.